# Iron Binding, a New Function for the Reticulocyte Endosome $H^+$-ATPase†

Cai-Yuan Li,* J. Abra Watkins, Shuji Hamazaki,‡ James D. Altazan, and Jonathan Glass

*Department of Medicine, Hematology/Oncology Division, Center for Excellence in Cancer Research, Treatment, and Education, Louisiana State University Medical Center, 1501 Kings Highway, Shreveport, Louisiana 71130-3932*

*Received September 29, 1994; Revised Manuscript Received January 6, 1995*⊗

ABSTRACT: The significance of the $H^+$-ATPase in iron absorption by rabbit reticulocytes is explored using isolated endosomes, effects of inhibitors, and the purified proton pump. We have recently reported $H^+$-ATPase-mediated iron transfer across a liposomal membrane (Li et al., 1994). In this report, the effect of $H^+$-ATPase inhibitors on iron mobilization is investigated at pH 6.0 in the presence of 15 $\mu$M FCCP in order to dissociate $^{59}$Fe(III) from transferrin and eliminate the kinetic effects of acidification by the ATPase. Iron transport by isolated endosomes is decreased 50% by the cation pore inhibitor dicyclohexylcarbodiimide (DCCD) for ascorbate-mediated iron mobilization and increased by 40−50% when NADH and ferrocyanide are used as electron donors. In contrast, the ATPase hydrolysis inhibitors *N*-methylmaleimide (NEM) and 7-chloro-4-nitrobenz-2-oxa-1,3-diazole (NBD) increase iron mobilization when NADH and ferrocyanide are used as reductants but have negligible effects for ascorbate. The differential inhibition or enhancement by DCCD, NEM, and NBD with respect to the reductants used for mobilization indicates that the $H^+$-ATPase may be involved in the multiple pathways of iron transport found in isolated rabbit reticulocyte endosomes. Effects of inhibitors of ATP hydrolysis suggest significant structural interactions between the proton pump and sites for iron binding and/or reduction. The isolated $H^+$-ATPase binds iron as revealed by using nondenaturing electrophoretic and chromatographic methods. One class of iron binding sites is suggested to be the 17.5 kDa proton pore subunits of the $H^+$-ATPase which also covalently react with DCCD. Another class of iron binding sites appears to be near the nucleotide binding sites and inhibit hydrolysis. The putative proton pores bind iron when associated in a multimeric complex as extracted with toluene, but iron binding to dissociated or renatured individual subunits is not detected. It is suggested that the proton pores of the $H^+$-ATPase are one class of binding sites involved in iron mobilization by endosomes.

Iron uptake into cells proceeds through receptor-mediated endocytosis where diferric transferrin (Tf)[1] binds to the transferrin receptor ($R_{Tf}$) on the cell surface and is followed by internalization of the Tf−$R_{Tf}$ complex via coated vesicles (Jandl & Katz, 1963; Harding et al., 1983; Iacopetta & Morgan, 1983). Subsequent to endocytosis a number of steps are required for the release of iron from transferrin and transport of iron into the cytosol. These steps include acidification of the endosomal space, release of Fe(III) from transferrin, reduction of Fe(III) to Fe(II) within the endosome, and finally translocation of iron across the endosomal membrane to the cytosol (Nunez & Glass, 1983, 1985). It is possible to study the entire process of iron transport in endosomes isolated from rabbit reticulocytes. Activation of the $H^+$-ATPase acidifies the endosomal space to about pH 6.0, an acid milieu sufficient to dissociate Fe(III) from transferrin, while the addition of a reductant is required to mobilize Fe from the endosome (Nunez et al., 1990; Watkins et al., 1992a). As expected, inhibition of the hydrolytic activity of the proton pump with NEM or blocking the proton pore with DCCD inhibits acidification and Fe(III) dissociation from transferrin. It is possible to bypass the activity of the $H^+$-ATPase by suspending the endosomes at an acidic pH in the presence of the protonophore FCCP. In the acidic environment generated nonenzymatically, Fe(III) will dissociate from Tf and mobilization will occur if a reductant is present (Nunez et al., 1990; Watkins et al., 1992a). In the course of these later studies, we observed that, even with the acidification function of the $H^+$-ATPase bypassed, DCCD, the inhibitor of the proton pore, inhibited Fe(II) mobilization (Watkins et al., 1992a). The results and mechanistic considerations derived from kinetic analysis suggested that the $H^+$-ATPase may have a function in Fe transport that is not directly related to acidification. The results of analysis of reductant-dependent iron mobilization kinetics indicated multiple pathways of iron translocation following iron reduction, and the involvement of the $H^+$-ATPase was suggested (Watkins et al., 1992a). We have recently demonstrated that the $H^+$-ATPase reconstituted in liposomes can mediate the transport of ferrous iron (Li et al., 1994). The proteoliposome system provided additional support for the hypothesis that the $H^+$-ATPase is directly involved in iron transport *per se* irrespective of its role in endosomal acidification. The present studies were under-

† This work was supported by National Institutes of Health Grant DK-37866 and the Center for Excellence in Cancer Research, Treatment, and Education, Louisiana State University Medical Center.

* Corresponding author (telephone 318-675-5973; Fax 318-675-5944).

‡ Present address: Department of Pathology, Faculty of Medicine, Kyoto University, Sakyo-ku, Kyoto 606, Japan.

⊗ Abstract published in *Advance ACS Abstracts,* April 1, 1995.

[1] Abbreviations: $H^+$-ATPase, vacuolar proton-transporting ATPase; Tf, transferrin; $R_{Tf}$, transferrin receptor; ATP, adenosine 5′-triphosphate; FCCP, carbonyl cyanide *p*-(trifluoromethoxy)phenyl hydrazone; NADH, nicotinamide adenine dinucleotide; DCCD, *N,N*′-dicyclohexylcarbodiimide; NEM, *N*-ethylmaleimide; NBD, 7-chloro-4-nitrobenz-2-oxa-1,3-diazole; MES, 2-(*N*-morpholino)ethanesulfonic acid; EGTA, ethylene glycol bis(β-aminoethyl ether)-*N,N,N*′,*N*′-tetraacetic acid; PMSF, phenylmethane sulfonic acid; HEPES, *N*-(2-hydroxyethyl)piperazine-*N*′-2-ethanesulfonic acid; NTA, nitrilotriacetic acid.

0006-2960/95/0434-5130$09.00/0 

taken to explore the role of the $H^+$-ATPase in Fe transport and to determine if the $H^+$-ATPase isolated from rabbit reticulocyte endosomes could serve to bind iron.

## MATERIALS AND METHODS

*Vesicle Preparation.* Rabbit reticulocytes were generated in response to phenylhydrazine hydrochloride (Nunez & Glass, 1983, 1985), and endosomes were prepared as described (Nunez et al., 1990; Watkins et al., 1992a) with slight modifications. Cells were suspended in an equal volume of lysis buffer consisting of 50 mM 2-(*N*-morpholino)ethanesulfonic acid (MES) (pH 7.5), 0.5 mM $MgCl_2$, 1 mM EGTA, and 0.2 mM phenylmethanesulfonic acid (PMSF) and lysed by three cycles of freeze−thawing in liquid nitrogen and swirling in a 37 °C water bath. Each 2 mL of lysed suspension was sonicated for 15 s in a Model C112S bath-type sonicator (Lab Supplies Co. Inc.). The pooled suspensions were centrifugated for 30 min at 21 000 rpm using a Sorvall SS-34 rotor, and endosomes were further fractionated by layering 10 mL of supernatant onto a 50-mL Bio-Gel A 5.0 M column equilibrated with 100 mM NaCl, 1 mM EGTA, 0.5 mM $MgCl_2$, 0.2 mM PMSF, and 10 mM MES, pH 7.5 (elution buffer). The vesicles collected in the void volume were layered on a 30% Percoll cushion in the same buffer and further purified by centrifugation at 18 000 rpm for 50 min. The vesicle layer was carefully removed and centrifuged at 27 000 rpm for 1.5 h in a Beckman SW-28 rotor. The vesicle pellets were resuspended in MES elution buffer containing 10% glycerol. Vesicles prepared using these methods are highly enriched with regard to the quantity of $H^+$-ATPase relative to vesicles prepared at pH 7.0 in HEPES buffer used for iron mobilization studies (Watkins et al., 1992).

*Determination of ATPase Activity.* ATPase activity was determined by release of $[^{32}P]P_i$ from $\gamma$-$^{32}P$-labeled ATP as described (Stone et al., 1984; White & Ralston, 1976; Chen et al., 1984) with the incubation medium modified to consist of 100 mM MES (pH 6.5), 1 mM EGTA, 8 mM $MgCl_2$, and 3 mM ATP (100 000−200 000 cpm, diluted from [$\gamma$-$^{32}P$]-ATP, specific activity 3000 Ci/mmol).

*Purification of $H^+$-ATPase from Reticulocyte Endosomes.* Approximately 2 mg of vesicle protein was solubilized at 4 °C for 0.5 h in 1 mL of 1.5% octyl glucoside, 10% glycerol, and 25 mM Tris-HCl, pH 8.3. Usually, 0.5−0.8 mL of solubilized vesicles was layered in a 5 cm long well on top of a 2.5−16% polyacrylamide gradient gel [acrylamide/bis-(acrylamide)] containing 3.3% glycerol and 25 mM Tris-HCl, pH 8.3, and separated by electrophoresis overnight at 10 mA in a 0.2 M Tris−glycine buffer, pH 8.3. The $H^+$-ATPase activity was localized by incubation of a portion of the gel with 1 mM $Pb(CH_3CO_2)_2$ followed by incubation in 0.5% $Na_2S$ for 10 min (White & Ralston, 1976; Chen et al., 1984). The ATPase activity appears as a dark brown PbS precipitate. Under these conditions the $Na^+$,$K^+$-ATPase is not active. The proteins containing the ATPase activity were electroeluted from nonstained portions of the gel in an Elutrap (Schleicher & Schuell) for 24−48 h at 80 mA, 4 °C, in 0.2 M Tris−glycine (pH 8.3), 0.025% octyl glucoside or $C_{12}E_9$, and 4% glycerol. The yield of the eluted material was about 75.0 ± 9.8 $\mu$g/mg of vesicle protein. The proton pore was purified from the eluted material by extraction with toluene as described (Sun et al., 1987).

*Detection of $^{59}Fe$ Binding Activity in Purified $H^+$-ATPase.* Iron binding activity was assayed by two methods. In the first method, 1−5 $\mu$g of purified protein was loaded on a 2.5−16% nondenaturing polyacrylamide gel as above and transferred to nitrocellulose paper, and the previously described (Nunez et al., 1989) $^{59}Fe$ blotting technique was applied using 25 nM $^{59}Fe$ citrate (Fe:citrate 1:1000). In the second method, 1−5 $\mu$g of purified protein was incubated for 10 min at 4 °C in 50 $\mu$L with 5 nM $^{59}Fe$ citrate (1:1000 Fe:citrate), 0.025% octyl glucoside, and 10 mM HEPES, pH 5.0. The samples were diluted with 20 mM HEPES and 0.025% CHAPS, pH 7.0, loaded into a 100-$\mu$L or 250-$\mu$L HPLC injector loop, fractionated on a Dupont Zorbax GF-250 column, and eluted with 20 mM HEPES and 0.025% CHAPS, pH 7.0, running buffer at a flow rate of 1.0 mL/min. Eluted proteins were monitored using a Beckman 163 variable UV/vis detector at 285 nm and a Hewlett-Packard 89500 diode array spectrophotometer collecting full UV/vis spectra every 15 s. Eluted samples were collected and counted in a LKB Pharmacia 1282 $\gamma$ counter.

*Determination of Mobilization of $^{59}Fe$ from Endocytic Vesicles.* Mobilization of $^{59}Fe$ from the vesicles was determined as described (Nunez et al., 1990). Briefly, vesicles were isolated by incubating reticulocytes with $^{125}I$, $^{59}Fe$-labeled Tf prior to the preparation of vesicles using our previous isolation methods (Watkins et al., 1992a). Labeled vesicles were suspended at 37 °C in 10 mM HEPES, 50 mM NaCl, 50 mM KCl, 1 mM EGTA, 0.5 mM $MgCl_2$, and 15 $\mu$M FCCP, pH 6.0 (reaction buffer). At various times following the addition of solutions of reductants, aliquots of the vesicle solution (usually 125−250 $\mu$L containing a minimum of 10 $\mu$g of protein, 600 cpm $^{59}Fe$) were separated from the incubation solution containing mobilized $^{59}Fe$ by filtration through 0.22-$\mu$m Millipore GSWP filters.

## RESULTS

*Mobilization of $^{59}Fe$ from Reticulocyte Endosomes—Effect of DCCD, NEM, and NBD.* The effects of the proton pore inhibitor, *N,N'*-dicyclohexylcarbodiimide (DCCD), as well as the ATPase activity inhibitors, *N*-ethylmaleimide (NEM) and 7-chloro-4-nitrobenz-2-oxa-1,3-diazole (NBD), on iron mobilization by endosomes are shown in Table 1. In these experiments, concentrated vesicles (>1.5 mg/mL of vesicle protein) were incubated with a 50 $\mu$M inhibitor solution at pH 7.0, 37 °C, for 30 min prior to dilution of 100−250 $\mu$L of the vesicle suspension into 2 mL of pH 6.0 reaction buffer containing 15 $\mu$M FCCP for the filter assay and 1 mM ascorbate, 1 mM ferrocyanide, or 40 $\mu$M NADH. Under these conditions, the intravesicular pH is maintained at 6.0 and the requirement for ATP-mediated acidification is no longer necessary (Nunez et al., 1990; Watkins et al., 1992a); hence these conditions allow effects due to conformational and/or configurational changes to become revealed. Differential effects of the various inhibitors for a given reductant are demonstrated as well as differences between the effects of a given inhibitor between reductants. Significant heterogeneity among pathways of iron transfer is suggested by these results, and models in which the involvement of the $H^+$-ATPase in iron transfer processes is independent of its role as a proton pump are supported (Li et al., 1994; Watkins et al., 1992a).

The 50% inhibition of ascorbate-mediated mobilization in contrast to 25−50% stimulation of ferrocyanide-mediated

Table 1: Effects of $H^+$-ATPase Inhibitors, DCCD, NEM, and NBD, on Kinetic Parameters for Reductant-Dependent Iron Mobilization by Reticulocyte Endosomes[a]

| | | ascorbate (1 mM) | | NADH (40 $\mu$M) | | ferrocyanide (1 mM) | |
|---|---|---|---|---|---|---|---|
| reductant | | rate ($\times 10^{-3}$) and amplitude | % effect | rate ($\times 10^{-3}$) and amplitude | % effect | rate ($\times 10^{-3}$) and amplitude | % effect |
| control | $k_{obs}$ | 31.1 ± 5.0 | | 3.8 ± 0.8 | | 7.1 ± 0.4 | |
| | % mob | 56 ± 6 | | 25 ± 7 | | 37 ± 6 | |
| DCCD | $k_{obs}$ | 16.3 ± 2.0 | (−) 47 ± 14 | 2.8 ± 0.5 | (−) 26 ± 19 | 9.9 ± 1.1 | (+) 39 ± 8 |
| | % mob | 30 ± 3 | (−) 46 ± 10 | 24 ± 3 | (−) 4 ± 20 | 57 ± 7 | (+) 54 ± 14 |
| NEM | $k_{obs}$ | 30.8 ± 1.5 | (−) 1 ± 10 | 5.7 ± 0.9 | (+) 50 ± 18 | 6.6 ± 0.7 | (−) 7 ± 8 |
| | % mob | 53 ± 5 | (−) 5 ± 10 | 50 ± 10 | (+) 100 ± 24 | 51 ± 7 | (+) 37 ± 15 |
| NBD | $k_{obs}$ | 33.4 ± 1.8 | (+) 7 ± 11 | 5.1 ± 0.7 | (+) 34 ± 17 | 8.9 ± 0.7 | (+) 25 ± 7 |
| | % mob | 54 ± 6 | (−) 3 ± 11 | 54 ± 4 | (+) 116 ± 17 | 49 ± 5 | (+) 32 ± 13 |

[a] Estimate ±SD of at least three experiments. Estimates of observed rate constant, $k_{obs}$ ($\times 10^{-3}$ $s^{-1}$), and amplitude, % mob, were determined from nonlinear regression analysis using single-exponential curves (Watkins et al., 1992a). Enhancement (+) or inhibition (−) of the kinetics by the inhibitors is expressed relative to the control.

mobilization by DCCD suggests that the $H^+$-ATPase proton pore may be involved in one of the iron transit routes. Alternatively, a different endosomal protein with a structural motif similar to the $H^+$-ATPase proton pore may be involved in intermolecular iron transfer, reduction, or translocation (Watkins et al., 1992a). For either or both situations, the differential effect of DCCD on the rate and amount of iron mobilization indicates that iron reduction leading to extravesicular release follows a different route when mediated by ascorbate than for NADH or ferrocyanide. The kinetic parameters for ascorbate-mediated mobilization are insensitive to the effects of NEM or NBD in contrast to the enhancement of rates and/or amounts of NADH- and ferrocyanide-mediated iron mobilization (Table 1). Conformational coupling between the ATP hydrolysis sites of the $H^+$-ATPase and the routes of iron transfer and/or interactions between the $H^+$-ATPase and the oxidoreductase(s) mediating NADH and ferrocyanide electron transfer are suggested. In contrast, Fe(III) reduction by ascorbate is not affected by these ATPase inhibitors, suggesting direct reduction of Fe(III) by ascorbate on the intravesicular surface. Overall, the effects of DCCD, NBD, and NEM support models involving the $H^+$-ATPase in multiple routes of iron transfer and Fe(III) reduction leading to mobilization (Li et al., 1994).

*Purification of $H^+$-ATPase.* Methods have been described for the purification of the $H^+$-ATPase from several organs (Xie & Stone, 1986; Arai et al., 1987a). Application of these methods to reticulocyte endosomes proved to be unsuccessful because of the smaller amount of starting material and losses in the initial steps of purification. Because of the high degree of association of the endosomal proteins including the $H^+$-ATPase (Nunez et al., 1989; Watkins et al., 1992b), preliminary experiments were conducted to identify detergents that might differentially solubilize the complex from the endosomes. The presence of solubilized $H^+$-ATPase was assayed by the ability to enter a nondenaturing polyacrylamide gel and to catalyze the hydrolysis of ATP as observed by the formation of $P_i$ as detected by $Pb(CH_3CO_2)_2$. The results of nondenaturing polyacrylamide gel electrophoretic fractionation of endosomes solubilized with octyl glucoside are shown in Figure 1. Coomassie blue staining detected several protein bands (Figure 1, gel A). Many of these bands had the ability to catalyze the formation of the brown, PbS precipitate as shown in Figure 1, gel B. However, the three major low-mobility bands had the same molecular weight distribution of polypeptides as shown in the silver-stained

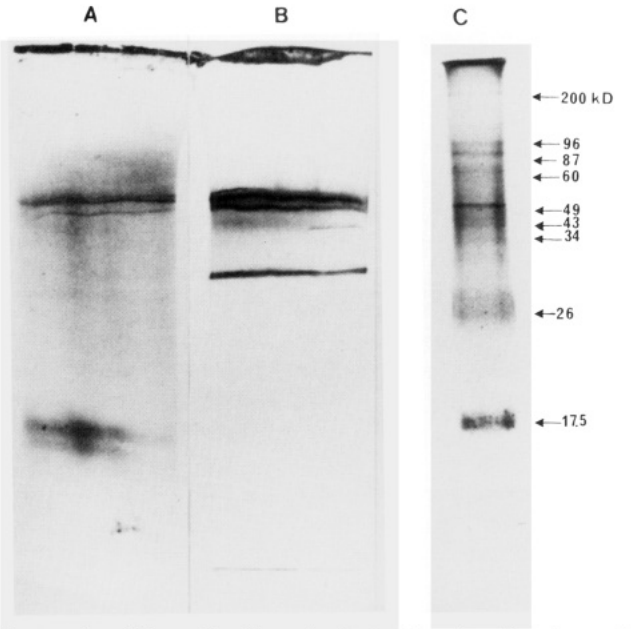


FIGURE 1: Polyacrylamide gel electrophoresis of endosomal proteins solubilized with octyl glucoside detergent demonstrating the presence and activity of $H^+$-ATPase. Approximately 50 $\mu$g of vesicle protein, solubilized with octyl glucoside, was subjected to nondenaturing polyacrylamide gel electrophoresis as described in Materials and Methods. Several protein bands were detected by Coomassie blue staining (gel A). ATPase activity was detected by lead sulfide precipitation as shown in the parallel gel (gel B). As described in Materials and Methods, proteins were electroeluted from the lowest mobility and most intense bands that entered the gel similar to those in gel B and were subjected to SDS−PAGE, $H^+$-ATPase polypeptides were detected using silver staining as shown in (C), and the molecular masses were assigned from molecular mass standards run in parallel.

SDS−PAGE result in Figure 1, gel C, indicating that multiple bands of ATPase activity shown in Figure 1, gel B, are derived from the same enzyme. It is reasonable to suggest that the multiple bands shown in Figure 1, gel B, are derived from multimers of the ATPase or result from heterogeneous association of phospholipids and/or detergent with the enzyme. It is important to note that under these conditions the $Na^+$,$K^+$-ATPase is not active (Li et al., 1991) since negligible inhibition by ouabain was observed as shown in Table 2. In addition, ouabain did not inhibit the $Pb(CH_3CO_2)_2$ reaction in the nondenaturing gel (Table 2). In similar experiments with Triton X-100, Triton X-114, and Nonidet

Table 2: Effects of ATPase Inhibitors on ATP Hydrolysis Activity by the Isolated $H^+$-ATPase[a]

| addition | inhibitor concn | ATP hydrolysis (% of control) |
|---|---|---|
| none | | 100 |
| NBD-Cl | 50 $\mu$M | 37.3 ± 25.9 |
| NEM | 50 $\mu$M | 31.9 ± 9.2 |
| oligomycin | 0.5 $\mu$M | 99.0 ± 0.5 |
| ouabain | 1 mM | 100.7 ± 0.9 |

[a] ATP hydrolysis was measured by release of [$^{32}$P]$P_i$ from [$\gamma$-$^{32}$P]ATP as described in Materials and Methods in the absence (control) or presence of the indicated reagents following incubation with 50 $\mu$M inhibitor at 37 °C for 30 min. The results expressed as a percentage of the activity of the control are the means ± SD of three experiments. The rate of hydrolysis in the absence of iron was 1036 ± 368 nmol of [$^{32}$P$P_i$ released $min^{-1}$ (mg of protein)$^{-1}$ for the isolated $H^+$-ATPase.

P-40, either ATPase activity was not detected or the sample did not migrate into the gel.

To further identify the ATPase activity as being the $H^+$-ATPase, proteins were electroeluted from nonstained gels that were run in parallel to a stained gel. Approximately 75 ± 10 $\mu$g of protein was recovered from 1 mg of endosomal protein (mean ± SE of eight experiments). The ATPase activity of the purified material was about 200−1000 nmol of ATP hydrolyzed $mg^{-1}$ $min^{-1}$, representing an enrichment of about 200-fold from the original endosomes. Consistent with vacuolar-type ATPase, activity was inhibited by NBD-Cl and NEM but was not inhibited by ouabain or oligomycin (Table 2). When the purified material was subjected to SDS−polyacrylamide electrophoresis, silver staining of the gel revealed nine proteins of molecular mass 200, 96, 87, 60, 49, 43, 34, 26, and 17.5 kDa as shown in Figure 1, gel C.

The purified $H^+$-ATPase was incubated with 50 $\mu$M [$^{14}$C]-DCCD at room temperature for 30 min. Upon extraction of the [$^{14}$C]DCCD-labeled purified ATPase with toluene (Sun et al., 1987), the $^{14}$C radioactivity was solubilized into the organic phase and subjected to nondenaturing electrophoresis, the gel was dried, and the autoradiogram indicated multiple protein bands as shown in Figure 2, gel B. The mobility of the intact purified ATPase, as detected by $Pb(CH_3CO_2)_2$, is shown in Figure 2, gel A, for comparison and is at a position similar to that of the ATPase activity shown in Figure 1, gel B. The multiple bands for the toluene-extracted fraction are identical in molecular mass as shown in Figure 3 and most likely represent multimers of the proton pore complex reminiscent of the multiple bands of the ATPase as found in Figure 1, gel B. Upon extraction of [$^{14}$C]DCCD-labeled purified ATPase with either (Sun et al., 1987) or chloroform−methanol (Arai et al., 1987b), the $^{14}$C radioactivity not only was solubilized into the organic phase but on SDS−polyacrylamide gel electrophoresis was consistent with a single protein band as detected by silver staining as shown in Figure 3. The molecular mass of the extracted fractions as well as the [$^{14}$C]DCCD-labeled band of the intact ATPase, as determined by SDS−polyacrylamide gel electrophoresis, was about 17 500 Da, tentatively identifying the DCCD binding activity as the proton pore protein.

*The $H^+$-ATPase of Reticulocyte Endosomes Binds $^{59}$Fe.* To determine if $^{59}$Fe binding activity resides in the $H^+$-ATPase, octyl glucoside solubilized endosomes and purified ATPase were subjected to electrophoresis on nondenaturing gradient gels, transferred to nitrocellulose paper, and assayed

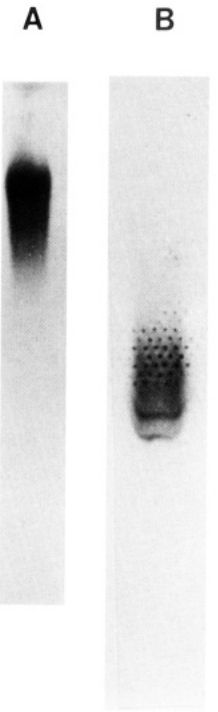


FIGURE 2: Autoradiogram of a nondenaturing gel indicating binding of the proton/cation pore inhibitor [$^{14}$C]DCCD to the purified $H^+$-ATPase, followed by toluene extraction of the radioactive fraction containing a protein with properties similar to those of the proton pore (gel B). The mobility of the intact purified ATPase, as detected by the $Pb(CH_3CO_2)_2$ reaction, is shown in gel A for comparison and is at a position similar to that shown in Figure 1, gel B. Nondenaturing gel electrophoresis conditions are identical to those described in Figure 1, the dot pattern in gel B is an artifact of the gel dryer, and the multiple bands behave as a single band under denaturing gel conditions as shown in Figure 3.

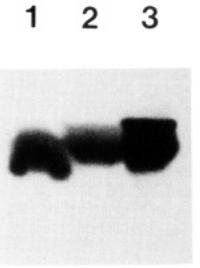


FIGURE 3: Silver stain of the SDS−polyacrylamide gel is shown for the 17.5 kDa subunit of the intact $H^+$-ATPase (lane 1), a fraction obtained by chloroform−methanol extraction (lane 2), and a fraction obtained by toluene extraction (lane 3) and demonstrates that the solubility properties of this subunit are similar to those of the proton pores of other V-type $H^+$-ATPases.

for $^{59}$Fe binding activity by incubation with $^{59}$Fe citrate at pH 5.0 (Nunez et al., 1989). As shown in Figure 4, only a single band of radioactivity was detected. No binding was detected if the purified material was subjected to SDS−PAGE (data not shown). Binding activity was also assayed by incubating the purified $H^+$-ATPase in solution with $^{59}$Fe at pH 5.0, followed by dilution into pH 7.0 buffer with subsequent analysis by HPLC gel filtration. As shown in Figure 5, $^{59}$Fe radioactivity was observed to elute as a single protein peak. On the basis of the specific activity of the $^{59}$Fe used, approximately four to five atoms of $^{59}$Fe elute per molecule of $H^+$-ATPase.

Due to our observation that $^{59}$Fe mobilization was inhibited by DCCD (Table 2), the ability of the proton pore protein

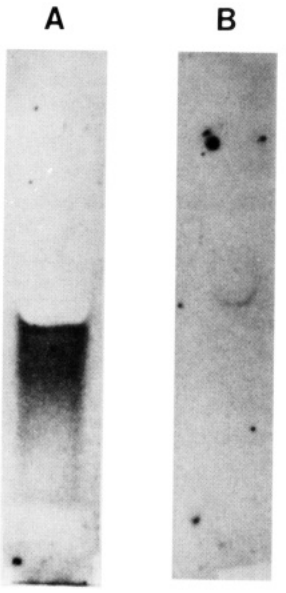


FIGURE 4: An autoradiogram of $^{59}$Fe binding to purified ATPase is shown following electrophoresis using a nondenaturing polyacrylamide gel, electroblotting on nitrocellulose paper, and incubation with $^{59}$Fe citrate (gel A). The sample in gel A was run further into the gel than similar samples shown in Figures 1 and 2. The autoradiogram of $^{59}$Fe binding to the toluene-extracted multimeric complex of 17.5 kDa proton pore subunits of purified ATPase after nondenaturating polyacrylamide electrophoresis, electroblotting to nitrocellulose, and incubation with $^{59}$Fe citrate is shown in gel B.

to bind $^{59}$Fe was examined. For these studies, purified ATPase was extracted with either toluene or chloroform−methanol, and the material extracted in the organic phase was fractionated on nondenaturing polyacrylamide gels, transferred to nitrocellulose paper, and blotted with $^{59}$Fe. An intact multimeric complex of the proton pores is obtained from the toluene extraction while chloroform−methanol yields partially denatured proton pore monomers (Sun et al., 1987; Arai et al., 1987b). Binding of $^{59}$Fe was observed only with the toluene extract (Figure 4, gel B). No binding was observed when either the toluene or chloroform−methanol extract was subjected to SDS−PAGE.

*Iron Effects on the Activity of the H$^+$-ATPase*. The above studies suggest that iron interacts with the proton pore; the binding of $^{59}$Fe to other constituents of the H$^+$-ATPase is difficult to evaluate since binding observed on nondenaturing gels was lost after SDS−PAGE. Hence, the effect of iron was assayed on the ATP hydrolysis activity of the isolated H$^+$-ATPase. As shown in Table 3, both iron(II) ascorbate and iron(III) citrate inhibited ATP hydrolysis in the presence of 8 mM $Mg^{2+}$, while no effect was seen with iron(III) NTA. Inhibition of ATP hydrolysis by iron(III) citrate also occurred with intact vesicles. In preliminary experiments, neither the $Na^+$ salt of citrate nor ascorbate at concentrations used in Table 3 inhibited the ATPase activity. The lack of effect of iron(III) NTA may reflect the higher affinity of NTA for Fe(III) relative to the affinity of citrate for Fe(III) as well as ascorbate for Fe(II). In addition, the H$^+$-ATPase may not have the ability to bind the iron(III) NTA complex. The apparent $K_i$ for the inhibition by Fe(III) and Fe(II) was approximately 5 $\mu$M. In similar experiments, $Ca^{2+}$, $Mg^{2+}$, and $Al^{3+}$ also inhibited hydrolysis. Optimal ATPase activity occurred at 0.5−2.0 mM $MgCl_2$ but decreased at higher concentrations with an apparent $K_i$ of approximately 8 mM. In the presence of 1 mM $MgCl_2$, the apparent $K_i$ for $CaCl_2$ was about 600 $\mu$M and 40 $\mu$M for $AlCl_3$.

## DISCUSSION

The H$^+$-ATPase of endosomes belongs to a class of vacuolar proton pumps that acidify intracellular compartments such as endosomes and lysosomes. The acidification of endosomes carrying Fe−Tf appears to be requisite for at least two functions in iron delivery to cells. First, an acidified millieu is required for Fe(III) to dissociate from

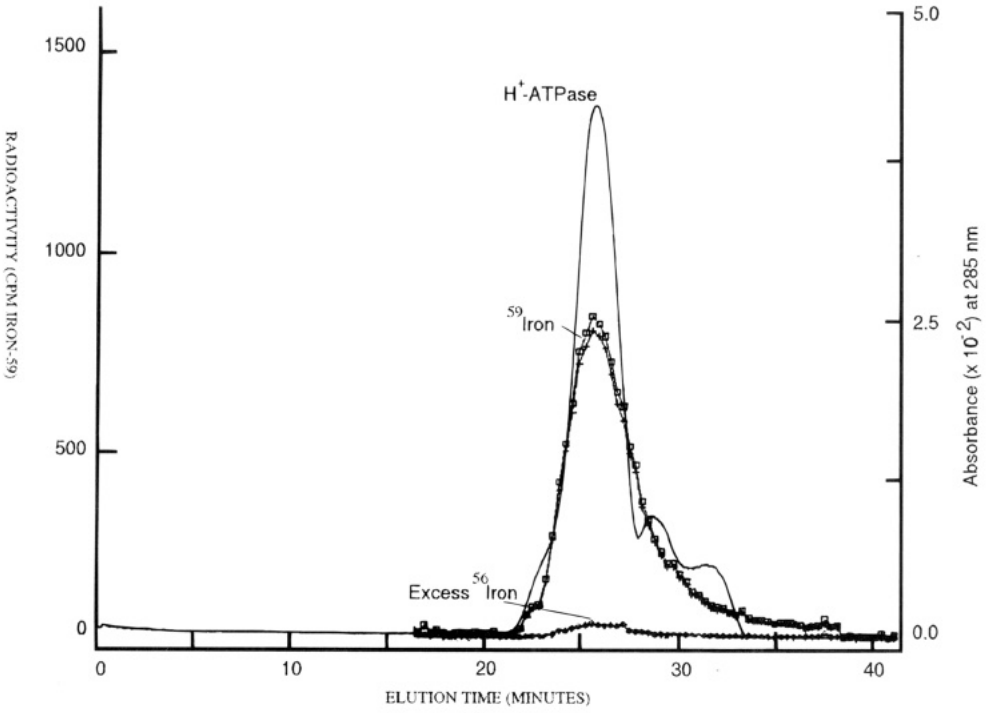


FIGURE 5: HPLC elution profile of purified ATPase is shown following incubation with 25 nM $^{59}$Fe citrate, indicating iron binding as detected by $^{59}$Fe radioactivity eluting with the main ATPase peak as detected by absorbance at 285 nm. The $^{59}$Fe radioactivity can be removed by incubation with excess (250 $\mu$M) cold iron citrate.

Table 3: Effect of Iron on ATP Hydrolysis by Isolated $H^+$-ATPase or $H^+$-ATPase in Vesicles[a]

| | % inhibition | | | |
|---|---|---|---|---|
| iron concn ($\mu$M) | 0 | 6 $\mu$M | 12 $\mu$M | 32 $\mu$M |
| iron(III) citrate | 100 | 53 ± 10 | 30 ± 3 | 25 ± 4 |
| iron(II) ascorbate | 100 | 54 ± 5 | 41 ± 8 | 35 ± 10 |
| iron(III) NTA | 100 | 129 ± 16 | 124 ± 6 | 95 ± 11 |
| iron(III) citrate in vesicles | 100 | 62 ± 11 | 47 ± 7 | 31 ± 5 |

[a] Ten micrograms of isolated $H^+$-ATPase protein purified as described in Materials and Methods was assayed for ATPase activity by release of $[^{32}P]P_i$ from [$\gamma$-$^{32}$P]ATP (Stone et al., 1984) except where 50 $\mu$g of vesicles was substituted as indicated. Reactions were conducted in a buffer containing 100 mM MES, 1 mM EGTA, and 8 mM $MgCl_2$, pH 6.5, at 37 °C with 3 mM ATP. Iron was added at the indicated concentrations at an iron to anion ratio of 1:1000 for citrate, 1:50 for ascorbate, and 1:4 for NTA to maintain iron solubility. The rate of ATP hydrolysis was expressed as a percentage of no added iron and is the mean ±SD of five experiments. The rate of hydrolysis in the absence of iron was 1036 ± 368 nmol of $[^{32}P]P_i$ released $min^{-1}$ (mg of protein)$^{-1}$ for the isolated $H^+$-ATPase.

Tf. Second, in an acidified milieu the now apo-Tf will stay bound to the $R_{Tf}$ and will recycle via exocytosis to be released from the cell, conserving the Tf for reutilization. We have recently developed a method for isolating endosomes from rabbit reticulocytes carrying $Fe_2Tf-R_{Tf}$ complexes (Choe et al., 1989; Nunez et al., 1990). In these endosomes, the entire process of iron delivery occurs, including dissociation of Fe(III) from Tf, reduction of Fe(III) to Fe(II), and the translocation of Fe(II) across the endosomal membrane to the extravesicular space. Acidification of the intravesicular space is a necessary first step in the process but can be bypassed by suspending the endosomes in buffer at pH 6 in the presence of a protonophore (Nunez et al., 1990; Watkins et al., 1992a). Under these conditions, Fe(III) dissociates from Tf to the same extent as if acidification were mediated by the proton pump. In addition, the effects of inhibitors of the $H^+$-ATPase on iron transport can be attributed to conformational and/or configurational changes related to iron transfer *per se* rather than their direct effect on acidification (Watkins et al., 1992a).

In the course of investigating possible inhibitors of the reduction or translocation steps, we noted that DCCD significantly affected mobilization of $^{59}$Fe under the conditions in which the need for the proton pump had been circumvented (Watkins et al., 1992a). As DCCD is known to interact with the 17.5 kDa subunit or proton pore of the vacuolar $H^+$-ATPase (Arai et al., 1987b; Sun et al., 1987), the observed inhibition suggested that a component of the ATPase could be involved in the handling of iron. The effects of NEM and NBD-Cl have a more complex interpretation since these inhibitors covalently interact with the ATP hydrolysis sites on the extravesicular surface while affecting the iron transit route at intravesicular sites. The $H^+$-ATPase ratio previously determined (Gaete et al., 1991) indicates conformational coupling between the subunits for ATP hydrolysis and the proton translocating pore of the $H^+$-ATPase. Therefore, it is reasonable to propose that NEM and NBD-Cl perturb the iron occupancy or handling of iron by the proton pore. Alternatively, ATP hydrolysis inhibitors may affect the enzyme conformation and subsequent interactions of the $H^+$-ATPase with other enzymes and/or proteins involved in the transport or reduction of iron leading to mobilization. For either situation, the covalent inhibition of ATP hydrolysis sites by NEM and NBD-Cl perturbs the distribution of iron among binding sites and/or their availability to reducing equivalents provided by ascorbate, NADH, or ferrocyanide. In addition, the effects of DCCD suggest that these binding sites are likely to be the $H^+$-ATPase proton pore and are involved in processes leading to mobilization (Li et al., 1994).

While DCCD, is a lipophilic, carboxyl group-reactive agent that inhibits enzyme systems that translocate protons and other ions, it is possible that DCCD could interact with other endosomal proteins involved in iron mobilization such as a transmembrane NADH dehydrogenase or $Ca^{2+}$-ATPase (Murphy, 1981; Vuokila & Hassinen, 1988, 1989). To determine if iron interacts in any significant way with the reticulocyte $H^+$-ATPase, it was necessary to establish a method for isolating the proton pump of the reticulocyte endosomes. The yield of material obtained when described methods (Xie & Stone, 1986; Arai et al., 1987a) were applied to 20−40 mL of reticulocyte-rich blood was too small to be of practical use. Advantage was taken of the observation that the proton pump isolated from other tissues was approximately of molecular mass 600 000 Da and that the pump did not dissociate when solubilized with octyl glucoside. Hence, it was possible to separate the proton pump on a nondenaturing gradient gel, detecting ATP hydrolysis by the precipitation of lead with released phosphate. Under the conditions of the ATPase assay the $Na^+,K^+$-ATPase was inactive. Three observations suggest that the isolated material is the proton pump. First, the molecular mass distribution of peptides detected on subsequent SDS−PAGE is similar to that described for other vacuolar pumps (Arai et al., 1987a, 1988; Forgac, 1992). Second, the material binds [$^{14}$C]DCCD and in particular the DCCD binds to a protein of 17.5 kDa, similar to the molecular mass of DCCD binding proteins in other proton pumps. Finally, the spectrum of inhibition of the ATPase activity is similar to that seen with other pumps (Schneider, 1981, 1987; Galloway et al., 1983; Wang & Gluck, 1990; Gluck, 1992). These considerations and results presented here strongly suggest that the proton pore of the $H^+$-ATPase binds iron without regard to the complications usually associated with the interpretation of inhibitor studies.

In general, the results can be interpreted to indicate at least two classes of iron binding sites on the V-type $H^+$-ATPase. One group of iron binding sites appears to be on the proton pore complex, which has been suggested to be involved in the pathway of iron transport across endosomal and liposomal membranes (Li et al., 1994; Watkins et al., 1992a). The other group of sites appears to be at or near the regions of nucleotide hydrolysis, in agreement with reports on the effects of alkali and transition metals from other investigators (Wang & Gluck, 1990; Gluck, 1992; Xie & Stone, 1988). This latter class of sites might be suggested to be important for the regulation of endosomal acidification which has been proposed to be a significant factor in vesicular trafficking and transport (Fuchs et al., 1989; Cain et al., 1989). The former class of sites, the proton pores, is suggested here to be directly involved in processes leading to iron translocation although the exact role remains unclear. However, three lines of evidence strongly support such a proposal and indicate that (i) the isolated $H^+$-ATPase binds iron at subunits with properties very similar to the proton pores, (ii) the isolated ATPase reconstituted in liposomes will transport iron and can be inhibited by DCCD (Li et al., 1994), and (iii)

under conditions where endosomal acidification is circumvented, iron mobilization by intact endosomes can be inhibited or enhanced by compounds which chemically modify the $H^+$-ATPase. With regard to these considerations, the role of the proton pores in iron transport is being further investigated.

## REFERENCES


Arai, H., Berne, M., Terres, G., Puopolo, K., & Forgac, M. (1987a) *Biochemistry 26*, 6632−6638.

Arai, H., Berne, M., & Forgac, M. (1987b) *J. Biol. Chem. 262*, 11006−11011.

Arai, H., Terres, G., Pink, S., & Forgac, M. (1988) *J. Biol. Chem. 263*, 8796−8802.

Cain, C. C., Sipe, D. M., & Murphy, R. F. (1989) *Proc. Natl. Acad. Sci. U.S.A. 86*, 544−548.

Chen, J.-W., Sun, Q., & Huang, F. (1984) *Biochim. Biophys. Acta 777*, 151−154.

Forgac, M. (1992) *J. Bioenerg. Biomembr. 24*, 341−350.

Fuchs, R., Schmid, S., & Mellman, I. (1989) *Proc. Natl. Acad. Sci. U.S.A. 86*, 544−548.

Gaete, V., Nunez, M. T., & Glass, J. (1991) *J. Bioenerg. Biomembr. 23*, 147−160.

Galloway, C. J.; Dean, G. E., Marsh, M., Rudnick, G., & Mellman, I. (1983) *Proc. Natl. Acad. Sci. U.S.A. 80*, 3334−3338.

Gluck, S. L. (1992) *J. Bioenerg. Biomembr. 24*, 351−359.

Harding, C., Heuser, J., & Stahl, P. (1983) *J. Cell Biol. 97*, 329−339.

Iacopetta, B. J., & Morgan, E. H. (1983) *J. Biol. Chem. 258*, 9108−9115.

Jandl, J. H., & Katz, J. (1963) *J. Clin. Invest. 42*, 314−326.

Li, C.-Y., Hamazaki, S., Watkins, J. A., Altazan, J. D., & Glass, J. (1991) *FASEB J. 5*, A749.

Li, C.-Y., Watkins, J. A., & Glass, J. (1994) *J. Biol. Chem. 269*, 10242−10246.

Murphy, A. J. (1981) *J. Biol. Chem. 256*, 12046−12050.

Nunez, M. T., & Glass, J. (1983) *J. Biol. Chem. 258*, 9676−9680.

Nunez, M. T., & Glass, J. (1985) *J. Biol. Chem. 260*, 14707−14711.

Nunez, M. T., Pinto, I., & Glass, J. (1989) *J. Membr. Biol. 107*, 129−135.

Nunez, M. T., Gaete, V., Watkins, J. A., & Glass, J. (1990) *J. Biol. Chem. 265*, 6688−6692.

Schneider, D. L. (1981) *J. Biol. Chem. 256*, 3858−3864.

Schneider, D. L. (1987) *Biochim. Biophys. Acta 895*, 1−10.

Stone, D. K., Xie, X.-S., & Racker, E. (1984) *J. Biol. Chem. 259*, 2701−2703.

Sun, S.-Z., Xie, X.-S., & Stone, D. (1987) *J. Biol. Chem. 262*, 14790−14794.

Vuokila, P. T., & Hassinen, I. E. (1988) *Biochem. J. 249*, 339−344.

Vuokila, P. T., & Hassinen, I. E. (1989) *Biochim. Biophys. Acta 974*, 339−344.

Wang, Z.-Q., & Gluck, S. (1990) *J. Biol. Chem. 265*, 21957−21965.

Watkins, J. A., Altazan, J. D., Elder, P., Li, C.-Y., Nunez, M. T., Cui, X.-X., & Glass, J. (1992a) *Biochemistry 31*, 5820−5830.

Watkins, J. A., Abdul-Rahman, J. K., Altazan, J. D., Barton, J. B., Hamazaki, S., Li, C.-Y., & Glass, J. (1992b) *Biophys. J. 61*, A191.

White, M. D., & Ralston, G. B. (1976) *Biochim. Biophys. Acta 436*, 567−576.

Xie, X.-S., & Stone, D. K. (1986) *J. Biol. Chem. 261*, 2492−2495.

Xie, X.-S., & Stone, D. K. (1988) *J. Biol. Chem. 263*, 9859−9867.


BI9422945